Reprinted with permission from the publisher.
In: ETEP (European Transaction on Electrical Power) 1999.
Vol. 9, No. 5, pp. 285-291

Method for Detection and Location of Very High Resistive Earth Faults

S. Hänninen, M. Lehtonen

Abstract

A new method is presented for the detection and location of high resistive, permanent single-phase earth faults in medium-voltage (MV) distribution networks (20 kV). The systems considered are with unearthed or a compensated neutral and the fault resistances covered are in the range of 5 kΩ … 160 kΩ. The algorithms of the new method are based on the change of the neutral voltage and zero-sequence currents, measured at the MV substation and also at the distribution line locations.

1 Introduction

There are different ways of detecting and handling high impedance earth faults. The existing solutions can be classified as:

– direct measurement of the electric quantities of the power system [1–5],
– energy and randomness algorithms [6–7],
– harmonic analysis [8–9],
– artificial intelligence methods [10–11],
– neural networks [12],
– wavelet analysis [13–14] and
– chaotic pattern analysis [15].

This paper presents a new approach to the problem, based on the continuous monitoring of the changes of electric quantities, measured in the distribution system.

In the first part of the paper, the theory of earth faults in unearthed and compensated power systems is briefly presented. The main factors affecting high resistance fault detection are outlined and common practices for earth-fault protection in present systems are summarized.

The algorithms of the new method for high resistance fault detection and location are then presented. These are based on the changes of neutral voltage and zero-sequence currents, measured at the high-voltage /medium-voltage substation and also at the distribution line locations. The performance of the method is analyzed, and the possible error sources discussed. Among these are, for instance, switching actions, thunderstorms and heavy snowfall.

The feasibility of the method is then verified by an analysis based both on simulated data, which was derived using an EMTP-ATP simulator, and by real-system data recorded during field tests at three substations. For the error source analysis, some real-case data recorded during natural power-system events, is also used.

2 Networks with an Unearthed Neutral

In networks with an unearthed neutral, the currents of single-phase-to-ground faults depend mostly on the phase-to-ground capacitances of the lines. When the fault happens, the capacitance of the faulty phase is bypassed, and the system becomes unsymmetrical (**Fig. 1**). A model for the fault circuit can most easily

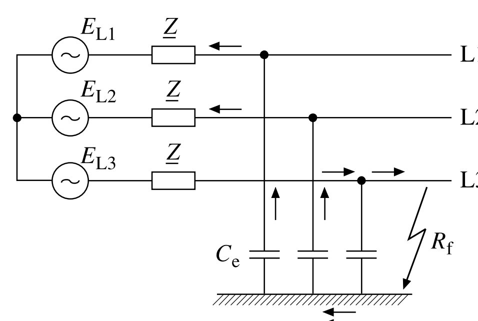

Fig. 1. Earth fault in a network with an unearthed neutral

be developed using *Thevenin*'s theorem. Before the fault, the voltage at the fault location equals the phase voltage E. The other impedances of the network components are small compared to those of the earth capacitances C_e, and can hence be neglected. This leads to the model in **Fig. 2**.

In the case where the fault resistance is zero, the fault current can be calculated as follows:

$$I_e = 3\omega C_e E, \quad (1)$$

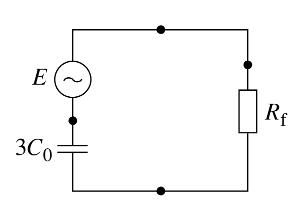

Fig. 2. Equivalent circuit for the earth fault in a network with an unearthed neutral

where $\omega = 2\pi f$ is the angular frequency of the network. The composite earth capacitance of the network C_e depends on the types and lengths of the lines connected in the same part of the galvanically connected network. In radially operated medium-voltage distribution systems this is, in practice, the area supplied by one HV/MV substation transformer.

In earth faults there is usually some fault resistance R_f involved, the effect of which is to reduce the fault current:

$$I_\mathrm{ef} = \frac{I_\mathrm{e}}{\sqrt{1+\left(\frac{I_\mathrm{e}}{E} R_\mathrm{f}\right)^2}}, \tag{2}$$

where I_e is the current obtained from eq. (1). In unearthed systems this does not, in practice, depend on the location of the fault. However, the zero-sequence current of the faulty feeder, measured at the substation, includes only that part of the current that flows through the capacitances of the parallel sound lines. The zero-sequence voltage U_0 is the same that the fault current causes when flowing through the zero-sequence capacitances:

$$U_0 = \frac{1}{3\omega C_0} I_\mathrm{ef}. \tag{3}$$

Using eqs. (1) and (2) this can also be written in the following form:

$$\frac{U_0}{E} = \frac{1}{\sqrt{1+(3\omega C_0 R_\mathrm{f})^2}}, \tag{4}$$

which states, that the highest value of neutral voltage is equal to the phase voltage. This value is reached when the fault resistance is zero. For higher fault resistances, the zero-sequence voltage becomes smaller. In networks with an unearthed neutral, the behaviour of the neutral voltage during the earth fault is of extreme importance, since it determines the overall sensitivity of the fault detection. Depending on the case, the highest fault resistance that can be detected using conventional relays is typically some kΩ.

3 Networks with a Compensated Neutral

The idea of earth-fault compensation is to cancel the system earth capacitances by an equal inductance connected to the neutral (**Fig. 3**), with a corresponding decrease in earth-fault currents. The equivalent circuit for this arrangement is shown in **Fig. 4**. The circuit is a

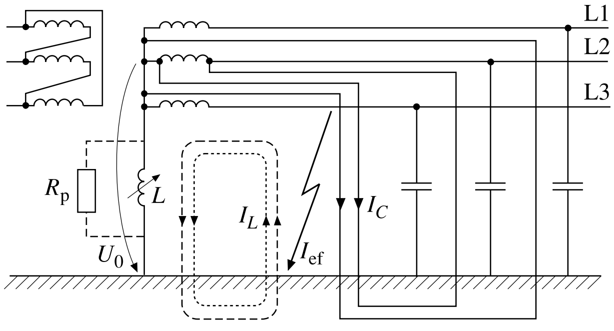

Fig. 3. Earth fault in a network with a compensated neutral

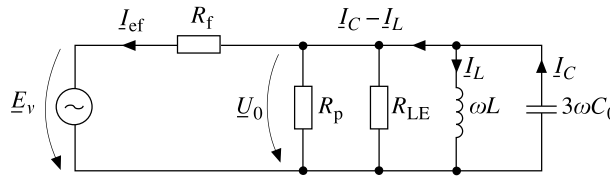

Fig. 4. Equivalent circuit for the earth fault in a network with a compensated neutral

parallel resonance circuit and if exactly tuned, the fault current has only a resistive component. This is due to the resistances of the coil and distribution lines together with the system leakage resistances (R_LE). Often the earthing equipment is complemented with a parallel resistor R_p, the task of which is to increase the ground fault current in order to make selective relay protection possible.

The resistive current is, in medium-voltage networks, typically from 5 % to 8 % of the capacitive current of the system. In totally cabled networks the figure is smaller, about 2 % to 3 % [16], whereas in networks with overhead lines solely, it can be as high than 15 % [17].

Using the equivalent circuit of Fig. 4, we can write for the fault current:

$$I_\mathrm{ef} = \frac{E\sqrt{1+R_\mathrm{LE}^2\left(3\omega C_0 - \frac{1}{\omega L}\right)^2}}{\sqrt{\left(R_\mathrm{f}+R_\mathrm{LE}\right)^2 + R_f^2 R_\mathrm{LE}^2\left(3\omega C_0 - \frac{1}{\omega L}\right)^2}}. \tag{5}$$

In the case of complete compensation, the above can be simplified as follows:

$$I_\mathrm{ef} = \frac{E}{R_\mathrm{LE}+R_\mathrm{f}}. \tag{6}$$

The neutral voltage U_0 can be calculated correspondingly:

$$U_0 = \frac{I_\mathrm{ef}}{\sqrt{\left(\frac{1}{R_\mathrm{LE}}\right)^2 + \left(3\omega C_0 - \frac{1}{\omega L}\right)^2}}, \tag{7}$$

which in the case of complete compensation, is reduced to the following form:

$$\frac{U_0}{E} = \frac{R_\mathrm{LE}}{R_\mathrm{LE}+R_\mathrm{f}}. \tag{8}$$

For the above equations it was assumed that no additional neutral resistor R_p is used. If needed, the effect of R_p can be taken into account by replacing R_LE in eqs. (5) to (8) by the parallel coupling of R_LE and R_p.

As in the case with an unearthed neutral, the highest zero-sequence voltage equals the phase voltage of the system. During earth faults, the neutral voltages are substantially higher in the systems with a compensated neutral than in the case with an unearthed one. Hence a more sensitive indication for high-resistance faults can be gained in the former case.

4 Present Techniques for Earth-Fault Detection

4.1 Earth-Fault Protection of MV feeders

The best result for earth-fault protection of MV lines in high-impedance earthed systems is gained by directional relays. In networks with an unearthed neutral, the phase shift between the earth-fault current of the faulty line and the current at the sound lines is about 180°. Hence, the selectivity is based on the measurement principle whereas the relay settings, neutral voltage and zero-sequence current, primarily affect the sensitivity of the protection only. In this case, the tripping is permitted, if the following conditions are met:

– the zero sequence current I_0 exceeds the setting, and

– the neutral voltage U_0 exceeds the setting, and

– the phase shift between I_0 and U_0 is in the range of $\varphi_0 + \Delta\varphi$ (where $\varphi_0 = 90°$ and $\Delta\varphi = \pm 80°$).

A more modern characteristic is the reactive current measurement, which is met in numerical relays. In this case the tripping is initiated, if neutral voltage and reactive current $I \sin\varphi$ both exceed the threshold value. However, in unearthed systems, there is practically no difference between the performance of the two relay characteristics, since the phase angle of the neutral voltage compared to the sum current is usually fairly close to –90°.

In resonant earthed systems, the protection cannot be based on the reactive current measurement, since the current of the compensation coil would disturb the operation of the relays. In this case, the selectivity can be based on the measurement of the active current component. Often the magnitude of this component is very small, and must be increased by means of a parallel resistor in the compensation equipment. The typical characteristics of the directional relays for compensated systems are similar to those used in unearthed networks. The only difference is that the characteristics are turned by –90°.

4.2 Use of Zero-Sequence Overvoltage Relays

In high-impedance earthed systems, the neutral voltage caused by an earth fault is practically the same in the whole supply area of the substation transformer. Also, its magnitude does not depend practically on the location of the fault. Consequently, a general detection of earth faults can be gained by means of a zero-sequence overvoltage relay.

In overhead line networks, faults with very high resistance can appear due to trees leaning against a conductor, for instance. These faults tend to evolve gradually into a fully established earth fault. A sensitive detection of such a fault can, to some degree, be achieved by neutral voltage relays. In this case, the voltage threshold should be as low as possible. The lowest limit depends on the neutral voltage present during the normal operating state. In unearthed systems this usually is very small, typically around 1 % of the nominal phase voltage, whereas in completely compensated networks higher values are encountered. In the latter case, the neutral voltage can be kept low by careful transposing of lines and by an appropriate setting of the compensation reactor. If the normal value varies below 2 %, a recommended relay setting is 3 %. In addition, a long time delay, up to 5 min, is needed. According to [18], these settings allow for the fault-detection sensitivity given in **Tab. 1**. It should be noted, however, that the settings in the example are applicable for alarm only.

U (in kV)	I_C (in A)	I_R (in A)	R_f (in kΩ)
6.6	5	5	13
11	5	5	22
22	10	10	22
33	20	10	24
44	20	10	32
55	20	10	40

Tab. 1. Sensitivity of earth-fault detection based on the zero-sequence overvoltage relay in a compensated system (U nominal voltage; I_C capacitive fault current after compensation; I_R resistive current of the system; R_f fault resistance value for which a fault can be detected [18])

The typical resistance of a tree is in the range of 20 kΩ … 80 kΩ. These figures apply in the seasons when the earth is not frozen. In the winter time much higher resistances, ranging up to several hundred kΩ are encountered. As can be noticed from Tab. 1, most faults of this type are beyond the reach of the zero-sequence overvoltage relays.

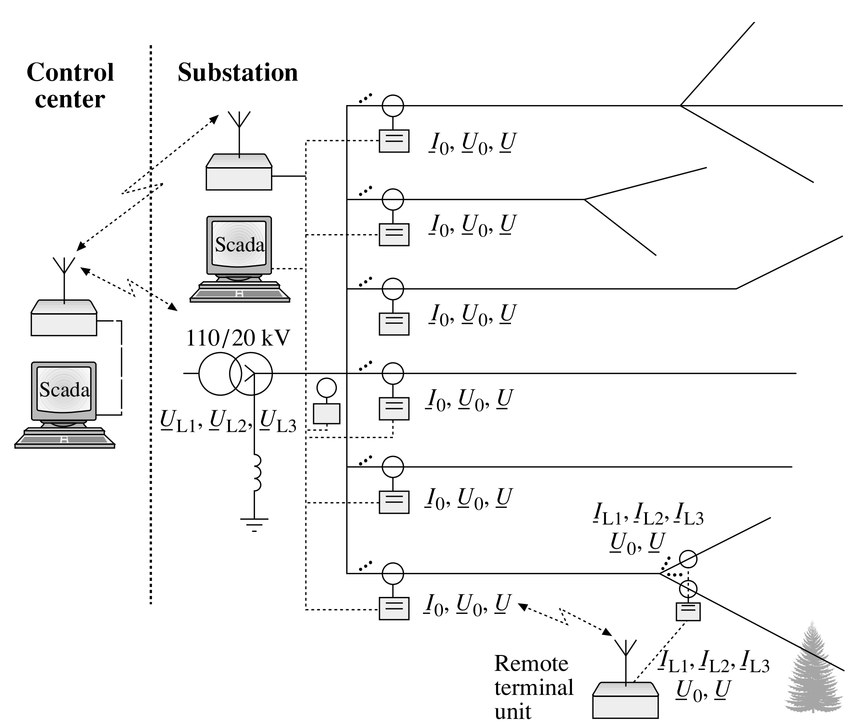

Fig. 5. High resistance fault-detection and location system

5 New Method for High Resistance Fault Detection

A new method for high resistance fault detection and location, based on the change of neutral voltage and zero-sequence currents, is presented in this section. The method consists of two independent and redundant algorithms, called neutral-voltage analysis and residual current analysis. The practical implementation of the method requires a close integration of the substation Scada with modern relays which are designed to be used for protection and control of the distribution network. A close connection is needed to the remote terminal units in the line locations as well (**Fig. 5**).

5.1 Neutral Voltage Analysis

The neutral voltage analysis algorithm can be explained by the simplified equivalent circuit for the one-phase earth fault (**Fig. 6**).

Using the equivalent circuit, the fault impedance $\underline{Z}_{\mathrm{f}}$ can be determined in terms of the measured voltages and the zero-sequence impedance of the network as follows:

$$\underline{Z}_{\mathrm{f}} = \left(\frac{\underline{U}_1}{\underline{U}_0} - 1\right)\underline{Z}_0 \,. \tag{9}$$

$\underline{Z}_0$ can be determined from the equivalent circuit of **Fig. 7**. In the unearthed network (Fig. 7a) it is the parallel connection of the phase-to-ground capacitances and phase-to-ground resistances, the so called "leakage resistances". For systems earthed via a Petersen coil, the circuit must be complemented with parallel connection of the coil impedance (Fig. 7b).

For the detection of a high resistance earth fault it is essential to determine the resistive part of the fault impedance. In eq. (9), $\underline{U}_0$ represents the phasor sum of the phase voltages and $\underline{U}_1$ is the positive sequence component of the phase voltage, measured at the moment considered. Applying eq. (9) for three times and using for $\underline{U}_1$ the following values: $\underline{U}_1$, $\underline{a}\,\underline{U}_1$ and $\underline{a}^2\underline{U}_1$, the faulted phase can also be determined. Here $\underline{a}$ is the phase shift operator, $\underline{a} = \mathrm{e}^{\mathrm{j}120°}$.

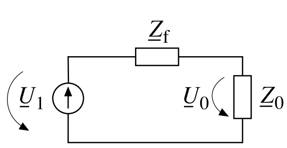

Fig. 6. Simplified equivalent circuit for an earth fault in a distribution network

From the calculated three values of $\underline{Z}_{\mathrm{f}}$, the resistive part shows the highest value in the faulted phase. Because the fault impedance must be resistive, the calculated resistive parts of $\underline{Z}_{\mathrm{f}}$ for the other two "healthy" phases are negative. The triggering level of the algorithm is set so that a high resistive earth fault is indicated, if the calculated maximum real part of $\underline{Z}_{\mathrm{f}}$ is smaller than the fixed threshold value and is at least four times the magnitude of the imaginary part of the corresponding $\underline{Z}_{\mathrm{f}}$.

The detection of very high fault resistances is difficult due to the neutral voltage present in the normal network conditions. This is mainly caused by the natural unbalances of the feeders. The sensitivity of the method can be improved by using the change of the neutral voltage which is determined as a difference of the real neutral voltage in the network at the moment being considered and of the corresponding mean value of the last 10 min [19].

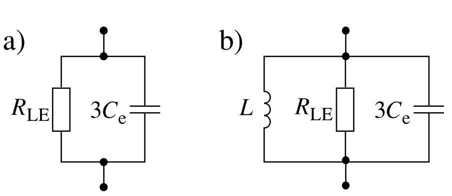

Fig. 7. Equivalent circuits
a) Zero-sequence network for the unearthed system
b) Compensated system

5.2 Residual Current Analysis

The faulted feeder is most often localised by the comparison of the residual current magnitudes. The indication is considerably more sensible, if the influence of the natural unbalances is eliminated by using the changes of the residual currents rather than the currents themselves. [4] introduces a method which uses the variations of the residual currents, neutral-to-ground voltage, phase-to-ground voltages and the values of the global phase-to-ground admittances of the feeders. It yields an estimate of the fault resistance and of the faulty phase correctly up to 100 kΩ.

The new algorithm presented in this paper utilises the simultaneous changes of neutral voltages and residual currents (**Fig. 8**). The idea of the algorithm is to compensate the effect of the earth capacitances using the measured change of the neutral voltage and the known zero-sequence impedance of the feeder considered (eq. (10)):

$$\Delta\underline{I}_{0j} = \Delta\underline{I}_{0j\mathrm{m}} - \frac{\Delta\underline{U}_{0\mathrm{m}}}{\underline{Z}_{0j}} \,. \tag{10}$$

Depending on the measuring accuracy, the resulting compensated current of a healthy feeder is nearly zero and in the case of the faulty feeder, it corresponds to one third of the earth fault current at the fault point. This method can also be used to discriminate the faulty line section, if the disconnector stations are provided with modern remote terminal units.

This method requires accurate knowledge about the zero-sequence impedances of each feeder. An advantage of the method is that, in the case of autoreclosure, the modern relays restore the values of the neutral volt-

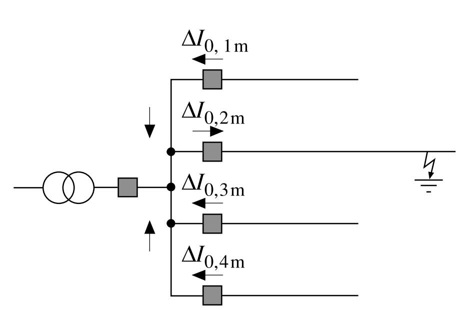

Fig. 8. Flows of the zero-sequence currents in the case of the earth fault

age and zero-sequence currents in the healthy feeders. These values can be used to update the zero-sequence impedance data.

After calculation of the fault resistance, the fault current can also be determined using the equivalent circuit of Fig. 6. When combining this information with the knowledge of the compensated zero-sequence currents and of the faulty phase, a very powerful means for detecting the faulty feeder, and further the faulty branch of the line, can be implemented.

6 Feasibility of the Method and Error Sources

In order to expose the detection algorithms to a wide range of field conditions, the algorithms were tested with naturally occurring faults, intermittent disturbances, staged faults and normal system activity. The feasibility of the method was also verified by an analysis based on simulated data, derived using an EMTP-ATP based network model. In the simulations, the sampling rate was 500 Hz and the sampling period was 1 s. Using simulated data, earth faults up to 500 kΩ could be detected. In order to evaluate the accuracy of the algorithm, we must keep in mind, that the simulated data did not include error factors. Among these are: the noise of the measured quantities produced by the power system itself, the accuracy of the measurement transducers, the properties of the electrical circuits of the measuring system, etc. [20].

Staged fault		Lammi		Maalahti		Kitee	
R_f (in kΩ)	Ph.	R_{fc} (in kΩ)	arg ($\underline{Z}_f$)	R_{fc} (in kΩ)	arg ($\underline{Z}_f$)	R_{fc} (in kΩ)	arg ($\underline{Z}_f$)
20	L1	15.9	8.6°	20.5	11.3°	17.0	−7.2°
40	L2	39.8	7.6°	41.7	2.1°	26.4	−10.1°
60	L3	71.2	1.8°	62.2	10.5°	46.8	−2.9°
80	L2	83.0	7.6°	80.5	−1.1°	50.2	−10.1°
100	L1	111.8	6.9°	131.3	5.5°	81.5	−14.8°
160	L3	179.5	−7.6°	120.0	18.7°	142.4	−3.0°
180	L3	177.0	−33.6°	141.6	17.2°	156.6	−0.9°
220	L3	178.1	−40.6°	223.3	27.0°	194.4	−2.4°
Tree	L1	174.4	9.4°	–	–	–	–
Tree	L1	207.1	7.0°	–	–	–	–
Tree	L2	281.9	33.3°	–	–	–	–
Tree	L3	237.8	−32.0°	–	–	–	–

Tab. 2. Experimental results obtained by the neutral voltage algorithm (R_f real fault resistance: Ph. faulty phase in the field test; R_{fc} calculated fault resistance (real part of the fault impedance); arg ($\underline{Z}_f$) argument of the fault impedance (in degrees))

Staged fault		Substation					Disc.
R_f (in kΩ)	Ph.	$3\Delta I_{01m}$ (in A)	$3\Delta I_{02m}$ **(in A)**	$3\Delta I_{03m}$ (in A)	$3\Delta I_{04m}$ (in A)	$3\Delta I_{05m}$ (in A)	$3\Delta I_{0m}$ **(in A)**
20	L1	0.284	**0.467**	0.227	0.599	0.569	**0.318**
40	L3	0.157	**0.421**	0.149	0.384	0.390	**0.228**
60	L2	0.108	**0.284**	0.091	0.248	0.239	**0.141**
80	L3	0.082	**0.152**	0.062	0.175	0.170	**0.099**
100	L2	0.054	**0.105**	0.069	0.182	0.178	**0.090**
120	L3	0.045	**0.069**	0.042	0.109	0.097	**0.054**
160	L1	0.010	**0.093**	0.043	0.137	0.139	**0.090**
180	L2	0.039	**0.036**	0.047	0.134	0.127	**0.084**
200	L1	0.034	**0.063**	0.047	0.125	0.110	**0.042**
220	L1	0.021	**0.049**	0.025	0.057	0.055	**0.069**

Tab. 3. Changes of the measured residual currents in the beginning of the feeders at the Kitee substation and at the disconnector location (faulted feeder is marked in boldface)

Staged fault		Substation					
R_f (in kΩ)	Ph.	$3\Delta I_{01}$ (in A)	$3\Delta I_{02}$ (in **A**)	$3\Delta I_{03}$ (in A)	$3\Delta I_{04}$ (in A)	$3\Delta I_{05}$ (in A)	$3\Delta U_{0m}$ (in V)
20	L1	0.047	**0.561**	0.010	0.019	0.017	1 350
40	L3	0.053	**0.545**	0.019	0.047	0.056	866
60	L2	0.029	**0.345**	0.056	0.025	0.027	574
80	L3	0.036	**0.191**	0.006	0.015	0.014	422
100	L2	0.015	**0.197**	0.012	0.034	0.032	365
120	L3	0.010	**0.095**	0.007	0.027	0.018	242
160	L1	0.027	**0.157**	0.010	0.026	0.028	201
180	L2	0.035	**0.114**	0.022	0.064	0.061	204
200	L1	0.050	**0.120**	0.026	0.069	0.059	154
220	L1	0.006	**0.072**	0.005	0.003	0.001	130

Tab. 4. Some experimental results for detection of the faulted feeder in a compensated network obtained by the residual current algorithm (faulted feeder is marked in boldface)

The field tests with staged faults were carried out in the normal network conditions at the Lammi substation of Häme Electricity and at the Maalahti substation of Vaasa Electricity, where the distribution networks are unearthed and at the Kitee substation in North-Carelian Electricity, where the network is compensated. The networks are mainly of overhead construction. **Tab. 2** to **Tab. 4** show some results of the earth fault test.

Tab. 2 shows the fault resistances determined by the neutral voltage algorithm from the field measurements at three substations and **Tab. 5** gives some corresponding values for the real case faults before they developed into a permanent fault. Especially in the compensated network, residual currents of the feeders are very low in the case of high-resistance earth faults. Tab. 3 shows the measured changes of the residual currents in the beginning of the feeders at the Kitee substation and at the disconnector location. The faulty feeder is marked in boldface. Tab. 4 shows some experimental results for detection of the faulty feeder in the compensated network obtained by the residual current algorithm. Our experience has shown that these algorithms are able to detect resistive earth faults reliably up to a resistance of 160 kΩ in a 20-kV distribution system.

Substation	Fault cause	R_f (in kΩ)
Honkavaara	Broken insulator	20.0
Honkavaara	Broken insulator	108.0
Honkavaara	Broken insulator	110.0
Honkavaara	Transformer fault	29.8
Honkavaara	Snow burden	29.2
Honkavaara	Snow burden	104.0
Kitee	Downed conductor	228.0
Lammi	Downed conductor	223.0
Renko	Tree contact	95.5

Tab. 5. Fault resistances detected by the neutral voltage algorithm before the fault developed into a permanent one

	Unearthed network			Compensated network		
	$R_{f,min}$ (in kΩ)	$R_{f,max}$ (in kΩ)	$R_{f,mean}$ (in kΩ)	$R_{f,min}$ (in kΩ)	$R_{f,max}$ (in kΩ)	$R_{f,mean}$ (in kΩ)
Switching action	43	199	93	10	218	53
Thunder-storm	85	116	93	–	–	–
Snowfall	199	268	233	46	318	136

Tab. 6. Fault resistances detected by the neutral voltage algorithm in the case of some intermittent disturbances in the network

The drawback of the algorithms is that the normal system activity and intermittent disturbances may cause changes to the neutral voltage and residual currents similar to the real faults in the feeders. **Tab. 6** shows the calculated resistances which correspond to the recorded changes of the neutral voltages in the case of normal switching actions, thunderstorms and snowfalls. These results are based on the continuous monitoring and recording of the neutral voltages at four substations during the period of one and a half years. For discrimination of the intermittent disturbances, the algorithms use 1 s mean values of the currents and voltages and for calculations of the corresponding changes, mean values of the last 10 min are used as a reference level. Thunderstorms and snowfalls can be discriminated by the fact, that they usually affect several feeders simultaneously.

7 Conclusions

A new method was presented for the single-phase-to-earth fault detection and location in high impedance earthed distribution systems. The method is able to detect faults up to 160 kΩ. The drawback of the method is that the normal system activity and intermittent disturbances may cause changes to the neutral voltage and residual currents similar to the real faults in the feeders. Examples of these are normal switching actions, thunderstorms and snowfall. This problem can be mitigated by using longer time average measurements for comparison when identifying the fault feeder or line section. The algorithms were verified by field tests and the first trial system implemented in modern relays and substation Scada will be installed during the autumn of 1999.

8 List of Symbols and Abbreviations

8.1 Symbols

$\underline{a}$, $\underline{a}^2$	complex rotation operators
C_e	phase-to-ground capacitance of the system
C_0	zero-sequence capacitance
E	phase-to-ground voltage at fault location
$E_{L1,L2,L3}$	fault moment phase-to-ground voltage
I_C	capacitive fault current
I_e	earth fault current
I_{ef}	earth fault current reduced by fault resistance
I_R	resistive current
$\Delta\underline{I}_{0j}$	compensated zero-sequence current of the feeder j
$\Delta\underline{I}_{0mj}$	measured change of zero-sequence current of the feeder j
L	coil inductance
R_{LE}	phase-to-ground resistance of the system
R_f	fault resistance
R_p	parallel resistor
U	nominal voltage (phase-to-phase voltage)
U_1	positive-sequence component of the phase-to-ground voltage
$U_{L1,L2,L3}$	phase-to-ground voltages
U_0	neutral voltage (zero-sequence voltage)
$\Delta\underline{U}_{0m}$	measured change of neutral voltage (zero-sequence voltage)
$\underline{Z}_0$	zero-sequence impedance of the network
$\underline{Z}_{0j}$	zero-sequence impedance of the feeder j
$\underline{Z}_f$	fault impedance
ω	rated angular frequency

8.2 Abbreviations

EMTP-ATP	electromagnetic transients program-alternative transients program
HV/MV	high voltage/medium voltage (substation)
Scada	supervision control and data acquisition

References

[1] *Aucoin, B. M.; Jones, R. H.:* High Impedance Fault Detection Implementation Issues. IEEE Trans. on Power Delivery PWRD-11 (1996) no. 1, pp. 139 – 148

[2] *Winter, K.:* Nollpunktsanalysis – ny metod att detektera högohmiga jordfel. ERA Electricitetens Rationella Använding (Sweden) (1988) no. 5, pp. 18 – 20 and 23 – 24

[3] *Leitloff, V.; Pierrat, L; Feuillet, R.:* Study of the Neutral-to-Ground Voltage in a Compensated Power System. ETEP Eur. Trans. on Electr. Power 4 (1994) no. 2, pp. 145 – 153

[4] *Leitloff, V.; Feuillet, R.; Griffel, D.:* Detection of Resistive Single-Phase Earth Faults in a Compensated Power-Distribution System. ETEP Eur. Trans. on Electr. Power 7 (1997) no. 1, pp. 65 – 73

[5] *Kim, C. J.; Russel, B. D.:* Analysis of Distribution Disturbances and Arcing Faults Using the Crest Factor. Electr. Power Syst. Res. 35 (1995) no. 2, pp. 141 – 148

[6] *Li, S.; Russel, B. D.:* Optimal Arching Fault Detection Using Signal Processing Techniques. Electr. Power Syst. Res. 21 (1991) no. 2, pp. 121 – 128

[7] *Benner, C.; Carswell, P.; Russel, B. D.:* Improved Algorithm for Arching Faults Using Random Fault Behavior. Electr. Power Syst. Res. 17 (1989) no. 1, pp. 49 – 56

[8] *Russel, B. D.; Mehta, K.; Chinchali, R. P.:* An Arching Fault Detection Technique Using Low Frequency Current Components – Performance Evaluation Using Recorded Field Data. IEEE Trans. on Power Delivery PWRD-3 (1988) no. 4, pp. 1 493 – 1 500

[9] *Jeerings, D. I.; Linders, J. R.:* Unique Aspects of Distribution System Harmonics Due to High Impedance Ground Faults. IEEE Trans. on Power Delivery PWRD-5 (1990) no. 2, pp. 1 086 – 1 094

[10] *Russel, B. D.; Chinchali, R. P.:* A Digital Signal Processing Algorithm For Detecting Arcing Faults on Power Distribution Feeders. IEEE Trans. on Power Delivery PWRD-4 (1989) no. 1, pp. 132 – 140

[11] *Russel, B. D.; Benner, C. L.:* Arcing Fault Detection for Distribution Feeders: Security Assessment in Long Term Field Trials. IEEE Trans. on Power Delivery PWRD-10 (1995) no. 2, pp. 676 – 683

[12] *Sultan, A. F.; Swift, G. W.; Fedirchuk, D. J.:* Detection of High Impedance Faults Using a Multi-Layer Perceptron. IEEE Trans. on Power Delivery PWRD-7 (1992) no. 4, pp. 1 871 – 1 876

[13] *Chaari, O.; Meunier, M.; Brouaye, F.:* Wavelets: A New Tool for the Resonant Grounded Power Distribution Systems Relaying. IEEE Trans. on Power Delivery PWRD-11 (1996) no. 3, pp. 1 301 – 1 308

[14] *Yinin, X.; Li, Q.; Wai, D. C. T.:* DSP Implementation of a Wavelet Analysis Filter Bank for High Impedance Fault Detection. Int. Conf. on Energy Managem. and Power Delivery (EMPD'98), Singapore, Proc. IEEE Cat. no. 98EX137, pp. 417 – 421

[15] *Ko, J. H.; Shim, J. C.; Ryu, C. W.; Park, C. G.; Yim, W. Y.:* Detection of High Impedance Faults Using Neural Nets and Chaotic Degree. Int. Conf. on Energy Managem. and Power Delivery (EMPD'98), Singapore, Proc. IEEE Cat. no. 98EX137, pp. 399 – 404

[16] *Hubensteiner, H.:* Schutztechnik in elektrischen Netzen. Offenbach · Berlin/Germany: VDE VERLAG, 1989

[17] *Claudelin, P.:* Compensation of the earth fault current in a MV distribution network. INSKO Insinöörijärjestöjen Koulutuskeskus 157-91 (Earth- Fault Problems in MV Systems), Helsinki/Finland 1991, Proc. pp. 1 – 38 (in Finnish)

[18] Känsliga jordfelsskydd: Bortkoppling av högresistiva jordslutningar i icke direkt jordade distributions- och transmissions system. Stockholm/Sweden: Svenska Eleverksföreningen, 1990

[19] *Lehtonen, M.:* A method for detection and location of high resistance earth faults in electrical distribution networks. Pat. FI. no 100922, ABB Transmit Oy, publ. 13.03.1998

[20] *Lehtonen, M.:* Transient analysis for ground fault distance estimation in electrical distribution networks. Espoo/Finland: VTT Publ. No 115, 1992

Manuscript received on April 6, 1998

The Authors

Seppo Hänninen (1956) has been with VTT Energy, Espoo, Finland, since 1987. His current position is research scientist in the research group, Electricity Distribution. He received his Master's degree in Electrical Power Engineering from Tampere University of Technology in 1980 and Licenciate degree in Electromechanics from Helsinki University of Technology in 1991. His main fields of interest are earth fault problems, distribution automation in medium voltage networks and reliability engineering. (VTT Energy, P.O. Box 1606, FIN-02044 VTT, Finland, Phone: +358 9 / 456 67 59, Fax: +358 9 / 456 65 38, E-mail: Seppo.Hanninen@vtt.fi)

Matti Lehtonen (1959) has been with VTT Energy, Espoo, Finland, since 1987 and since 1999 with Helsinki University of Technology, where he is a Professor of IT applications in power systems. He received his Master's and Licenciate degrees in Electrical Engineering, both from Helsinki University of Technology, in 1984 and 1989, respectively, and the Doctor of Technology degree from Tampere University of Technology in 1992. His main activities include earth fault problems, harmonic related issues and applications of information technology in distribution automation and distribution energy management. (Helsinki University of Technology, Power Systems Laboratory, P.O. Box 3000, FIN-02015 HUT, Finland, Phone: +358 9 / 451 54 84, Fax: +358 9 / 460 224, E-mail: Matti.Lehtonen@hut.fi)